XLI CILAMCE
XLI Ibero-Latin American Congress on Computational Methods in Engineering
16-19 November, 2020 FOZ DO IGUAÇU PARANÁ - BRAZIL

Multiscale approach for fatigue simulation in thermoplastic polymers

SILVA, J. V. A[1], FARIAS, J. M. C.[1], FANCELLO, E. A.[1]

[1]*GRANTE, Mechanical Engineering Department, Federal University of Santa Catarina*
Trindade, 88040-900, Florianópolis/ SC, Brazil
jvasilva13@gmail.com, janmichelfarias@gmail.com, eduardo.fancello@ufsc.br

Abstract. In mechanical engineering projects, mechanical fatigue is one of the most frequent sources of failure of devices submitted to cyclic loads.This is the case of orthopedic implants and prostheses, many of which are made of, or incorporate, polymeric materials. In large semi-crystalline polymers, mechanical fatigue is dominated by the nucleation process as a consequence of localized inelastic strain accumulation and craze formation. To simulate the local nucleation phenomenon in polymers, a multiscale model available in the literature was chosen, reproduced and his features analyzed and compared with experimental evidences. In this model it is considered an Representative Volume Element (RVE) composed by a matrix with a small volume fraction of ductile damaging inclusions. A homogenization scheme is formulated according to the Mean Field Homogenization (MFH) approach and the Mori-Tanaka solution. The mechanical behavior is limited to small deformations and disregards heat generation. The predictive fatigue life curves for High Density Polyethylene (HDPE) were reproduced and the contribution of this paper focuses on the sensitivity analysis of the model to load effects and inclusion material parameters.

Keywords: Fatigue, Thermoplastic, Multiscale

1 Introduction

According to Teoh [1], fatigue and wear fracture is identified as the main failure mode for metallic, ceramic and polymeric materials in different orthopedic applications. Under specific conditions of temperature and oscillatory loading, the fracture of a material occurs suddenly, without macroscopically change evidence in mechanical behavior. An example is the brittle failure in hip prostheses acetabular cup of UHMWPE. In these circumstances, mechanical behavior is speculated to start locally, fact that is evidenced by micrograph techniques applied to the specimens failure surface. The nucleation starts in microstructure random defects, originated by processing, such as microvoids and particulates. Classical metal failure theory cant describe the nucleation and microvoids growth, as as Mulla et al. [2] comments.

The nucleation process in thermoplastics is identified on regions with lower entanglement density. For semi-crystalline thermoplastics, these regions are at the interlamellar or interspherulite boundaries, as observed by Bessell et al. [3] and Bretz et al. [4]. To incorporate this concept in the macroscopic phenomenon, constitutive models with a multiscale approach are proposed. The term multiscale is applied to the dimensional scale, defined as the characteristic of associating microscopic mechanisms and macroscopic phenomena, through a mesoscopic or intermediate representation, called Representative Volume Element (RVE). Within this approach, several micromechanisms propositions to describe the local nucleation phenomenon and different methods to incorporate them in macroscopic simulations are found in the literature.

In fragile failure phenomenon, under high number of cycles, adequate choice of the multiscale approach is essential to reduce the simulation processing time. Provided that the analysis allows for necessary simplifications, the Mean-Field Homogenization (MFH) approach is much more efficient than homogenization Full-Filed Methods (FFM), because in specific circumstances the first presents a semi-analytical solution. This methodology has been largely applied to phisical phenomena that can be represented by a heterogeneous RVE, in with each material phase is uniform elastic and the inclusions are geometrically specific and simple. From these considerations, one idealization about the interaction between that phases is introduced by Mori-Tanaka solution which has others appropriate simplifications (details are seen in Mura [5]). There are different approaches to apply MFH theory in nonlinear constitutive relations.

Some propositions for nonlinear composites start from a first order homogenization like the Linear Comparison Composites (LCC) concept. In these methods, the constitutive model for the macroscopic scale and for each constitutive phase within the RVE are replaced by a linear approximation, with uniform instantaneous stiffness operator. Many linearization schemes can be applied according to the original nonlinear model mathematical structure. For some viscid materials models, Masson et al. [6] proposed the Affine Linearization method. The formulation is usually deduced in the Laplace-Carson domain, with constitutive relationship expressed by a linear fictitious thermoelastic model and the result needs to be mapped back to time domain. This comparison models are restricted to monotonic and proportional load, otherwise an incremental linearization method is required (Miled et al. [7]).

To simulate failure and predict high cycle fatigue life of HDPE under a complex load history, the work of Krairi et al. [8] applies the Incrementally Affine Linearization technique developed by Doghri et al. [9] in a rate-dependent model with damage. That formulation reduces the homogenization computational cost of rate-dependent materials and make it able to readily incorporate other effects. Their RVE have a matrix phase and very low volume fraction of weak spots prone to damaging, key concept idealized by the authors to simulate local failure. Therefore, in this study we propose to reproduce this model and contribute with a sensitivity analysis on load effects and weak spots parameters for expose applicability, difficulty and possible extensions.

2 Implicit Incremental Model

The material mesoscopic structure (intermediate scale) was based on the assumption that damage occurs in localized areas. For Krairi et al. [8] this structure admit the existence of weak spots that accumulate damage. This inclusions are modeled with spheroidal geometry and represent an RVE volume fraction small enough to not modify the macroscopic observable mechanical behavior. The authors' conception allows to simulate the progressive failure in the weak spots without macroscopic externalization of this phenomenon. Like a typical case of high cycle fatigue, there is no damage process macroscopic perception before crack propagation. Another RVE hypothesis implicitly involved is that the problem does not require microstructure fields description other than they average. Therefore, a first order homogenization method can be applied by comparison.

Fracture theory in thermoplastics holds similar assumptions for metals: nucleation mechanism starts and inelastic deformations concentration occurs simultaneously in regions with less entanglement density. Trying to reproduce this phenomenon, the weak spots are formulated according to a ductile damage model and rate influence is incorporated by a viscoelastic model coupled with viscoplastic constitutive relations. A thermodynamically consistent model is proposed by Krairi and Doghri [10]. The evolution equations are derived from a dual dissipation potential, based on the Generalized Standard Materials theory with von Mises criterion and Norton constitutive relation.As a limit case, the same model represents the viscoelastic behavior of the matrix phase and the macroscopic material. The equations are then numerically integrated using a fully implicit backward Euler scheme.

The incremental constitutive model of each phase was formulated for small deformation regime as in Krairi and Doghri [10]. This equations and Affine Linearization has similarities, they two involves a tangent operator and one more internal variable, called affine strain. The Incrementally Affine Linearization method developed by Doghri et al. [9] is a generalization of affine method, consistent with cited implicit integration. The MFH formulation for linear thermoelastics was used to define an appropriate and uniform stiffness tensor of the macroscopic material at each load increment. To this aim, the tangent operator in the original Affine Method is replaced by an algorithmic operator also consistent with proposed integration scheme.

Moreover, the Incrementally Affine Linearization technique allows the model to be reproduced by Eshelby's elastic and isotropic closed solution for a isolated inclusion in an infinite matrix. Mori-Tanaka's (MT) model is then applied to deduce MFH concentration tensors with the presence effects of other inclusions. This closed solution application directly on plasticity models leads too stiff predictions, because linearized constitutive relations has an anisotropic tangent stiffness. Alternatively a isotropic part can be extracted from that operator as proposed in Doghri et al. [9] who founds better results. Beside this, for nonlinear viscoplastic models the algorithm operator does not converge to analytical ones when time step decreases. This drawback was reported and worked around by authors [7–9] with a regularization equation.

2.1 Phase's constitutive model

Based on the thermodynamically consistent constitutive theory for dissipative materials, a Helmholtz potential ψ is proposed by Krairi and Doghri [10] as the sum of viscoelastic-viscoplastic accumulated energies, summarized in two contributions. The first one corresponds to the viscoelastic strain energy ψ^{ve}. and the other is viscoplastic flow resistance ψ^{h}. About damage, the strain energy ψ^{ve} is expressed as a function of an effective energy measure W^0 and a damage variable D. The second one ψ^{h} is represented by the sum of two hardening energies: Kinematic W^{kin} and isotropic W^{iso}. In Equation 1 and Equation 2, the energetic terms are expressed different from Krairi and Doghri [10] but they represent same model. This formulation we believe turn back some *ad hoc* made by the reference authors.

$$\psi = \psi^{ve} + \psi^{h} = (1-D)W^0 + W^{kin} + W^{iso} \tag{1a}$$

$$W^0 = \frac{1}{2}\boldsymbol{\epsilon}^{ve} : \mathbb{C}_\infty : \boldsymbol{\epsilon}^{ve} + \frac{1}{2}\sum \left(\boldsymbol{\epsilon}^{ve} - \boldsymbol{\epsilon}^{v}_{j}\right) : \mathbb{C}_j : \left(\boldsymbol{\epsilon}^{ve} - \boldsymbol{\epsilon}^{v}_{j}\right) \tag{1b}$$

$$W^{kin} = \frac{1}{2}\boldsymbol{X} : \boldsymbol{\alpha} = \frac{a}{2}\boldsymbol{\alpha} : \boldsymbol{\alpha} \tag{1c}$$

$$W^{iso} = \int_0^r R(z)dz = \int_0^r \kappa z^\theta dz \tag{1d}$$

The thermodynamic state is represented by the set $\boldsymbol{V} = \{\boldsymbol{\epsilon}, \boldsymbol{\epsilon}^{ve}, \boldsymbol{\epsilon}^{v}_{i}, \boldsymbol{\epsilon}^{vp}, \boldsymbol{\alpha}, r, D\}$ of state variables and their conjugates $\boldsymbol{A} = \{\boldsymbol{\sigma}, \boldsymbol{\sigma}_\infty, \boldsymbol{\sigma}_i, \boldsymbol{\mathcal{F}}, \boldsymbol{X}, R, -Y\}$. The evolution laws for the internal variables do automatically satisfy the Clausius-Plank positive dissipation by defining a convex dissipation potential $\check{\Phi}(\boldsymbol{A})$ given by the sum of the viscoelastic $\check{\Phi}^{ve}$ and viscoplastic $\check{\Phi}^{vpd}$ one coupled with damage contributions. The main concept underlying these definitions is the incorporation of the overstress in the potential. Then the accumulated deformation rate $\dot{r} = (1-D)\dot{p}$ can be found directly.

$$\check{\Phi}(\boldsymbol{A}) = \check{\Phi}^{ve} + \check{\Phi}^{vpd} \tag{2a}$$

$$\check{\Phi}^{ve} = \frac{1}{2}\sum \boldsymbol{\sigma}_j : \mathbb{V}_j^{-1} : \boldsymbol{\sigma}_j \tag{2b}$$

$$\check{\Phi}^{vpd} = \int_0^{f(\boldsymbol{A})} \frac{\omega(z)}{\eta_{vp}} dz \tag{2c}$$

$$\omega(f) = \eta_{vp}\dot{r} = \sigma_{y0}\left(\frac{f}{\sigma_{y0}}\right)^m \tag{2d}$$

This Viscoplasticity is a Perzyna based model that has overstress amplitude equal to the von Mises criterium f. Flow's rule depend on the backstress $\boldsymbol{X}$, isotropic hardening R and effective stress $\tilde{\boldsymbol{\sigma}}$. Other terms were introduced in the potential for Lemaitre-Chaboche damage and Armstrong-Frederick nonlinear kinematic hardening as well their respective dual potentials. Heaviside function $\mathcal{H}(p)$ determines whether damage is occurring, restricted to $p \geq p_D$. Material's failure occurs when $D \geq D_C$. The constitutive relation ω is a Norton Power law. All others variables are material parameters contained in the set $\mathcal{P} = \{\mathbb{C}_\infty, \mathbb{C}_i, \mathbb{V}_i, \sigma_{y0}, a, b, s, S, \kappa, \theta, m, \eta_{vp}, p_D, D_C\}$.

$$\begin{aligned} f = \sqrt{3J_2(\tilde{\boldsymbol{\sigma}} - \boldsymbol{X})} - \sigma_{y0} - R + \frac{b}{2a}J_2(\boldsymbol{X}) - \frac{ba}{2}J_2(\boldsymbol{\alpha}) \\ + \left[\frac{S}{s+1}\left(\frac{Y}{S}\right)^{s+1}\frac{\mathcal{H}(p)}{1-D}\right] - \left[\frac{S}{s+1}\left(\frac{\psi^{ve}(\boldsymbol{V})}{(1-D)S}\right)^{s+1}\frac{\mathcal{H}(p)}{1-D}\right] \end{aligned} \tag{3}$$

The energy model is these potentials which Helmholtz provides state laws for conjugates forces. Through the Generalized Normality Rule, internal variables evolution's laws are then obtained from the partial derivatives of the dissipation potential. The present formulation, the following set of independent state variables $\boldsymbol{Q} = \{\tilde{\boldsymbol{S}}, \boldsymbol{X}, r, D\}$ need to be updated at each time increment. Mises criterion simplify multi-axial plasticity in the second deviatoric scalar invariant J_2, consequently only the deviatoric effective stress part $\tilde{\boldsymbol{S}}$ has influence on plastic flow and the volumetric can be found directly by linear viscoelasticity.

$$\boldsymbol{Q}_{n+1} \approx \boldsymbol{Q}_n + \partial_t \boldsymbol{Q}_{n+1}\Delta t \tag{4}$$

Initial formulation are a complex system of non-linear differential equations as represented by the independent set $\boldsymbol{Q}$ in the continuum time domain. However, it was mentioned that the equations must be in incremental form according to a numerical integration. The homogenization method in next section requires implicit integration. In this approach, once determined Gateux derivative $\partial_t \boldsymbol{Q}$, it is possible to approximate a function $\boldsymbol{Q}_{n+1}$ at time t_{n+1} from the value known $\boldsymbol{Q}_n$ associated with the derivative evaluation at t_{n+1}. In Equation 4, this procedure is applied on $\boldsymbol{Q}$ and leads to the algebraic equations system $\boldsymbol{Q}_{n+1}$. The implementation solves this system by Newton's scheme and applies the Euclidean norm to verify the residue tolerance.

2.2 Linear comparison composite

Assuming a first order approach, the RVE was simplified to have phases $i = \{M, 1\}$ with uniform stiffness $\mathbb{C}_i^{alg}$ that represents the linear relationship between $\Delta\bar{\boldsymbol{\sigma}}_i$ and the phase strain $\Delta\bar{\boldsymbol{\epsilon}}_i$. The MFH theory determines a relation between the phase strain tensors $\Delta\bar{\boldsymbol{\epsilon}}_i$ and the respective macroscopic field $\Delta\bar{\boldsymbol{\epsilon}}$ through a volumetric mean. The approach proposed by Doghri et al. [9] was inspired by a similar correction used in linear thermoelasticity homogenization models. In Pierard et al. [11], the authors demonstrate how to obtain MFH formulation for linear thermoelasticity with the same concentration tensors $\mathbb{B}$ and $\mathbb{A}$ defined in elastic composites. This facilitates Mori-Tanaka elastic solution introduction when exist a affine strain term $\Delta\bar{\boldsymbol{a}}$ and correspondent stress $\Delta\bar{\boldsymbol{\varpi}}$.

$$\Delta\bar{\boldsymbol{\epsilon}} = (1 - v_1)\Delta\bar{\boldsymbol{\epsilon}}_M + v_1\Delta\bar{\boldsymbol{\epsilon}}_1 \tag{5a}$$

$$\Delta\bar{\boldsymbol{\epsilon}}_1 = \mathbb{A} : \Delta\bar{\boldsymbol{\epsilon}} + \Delta\bar{\boldsymbol{a}} = \mathbb{B} : \Delta\bar{\boldsymbol{\epsilon}}_M + \Delta\bar{\boldsymbol{a}} \tag{5b}$$

$$\Delta\bar{\boldsymbol{\sigma}}_M = \mathbb{C}_M^{alg} : \Delta\boldsymbol{\epsilon}_M + \Delta\bar{\boldsymbol{\varpi}}_M \tag{5c}$$

$$\Delta\bar{\boldsymbol{\sigma}}_1 = \mathbb{C}_1^{alg} : \Delta\boldsymbol{\epsilon}_1 + \Delta\bar{\boldsymbol{\varpi}}_1 \tag{5d}$$

$$\Delta\bar{\boldsymbol{a}} = (\mathbb{A} - \mathbb{I}) : (\mathbb{C}_1^{alg} - \mathbb{C}_M^{alg})^{-1} : (\Delta\bar{\boldsymbol{\varpi}}_1 - \Delta\bar{\boldsymbol{\varpi}}_M) \tag{5e}$$

$$\Delta\bar{\boldsymbol{\sigma}} = \bar{\mathbb{C}}^{alg} : \Delta\bar{\boldsymbol{\epsilon}} + \Delta\bar{\boldsymbol{\varpi}} \tag{5f}$$

$$\Delta\bar{\boldsymbol{\varpi}} = (1 - v_1)\Delta\bar{\boldsymbol{\varpi}}_M + v_1\Delta\bar{\boldsymbol{\varpi}}_1 + v_1(\mathbb{C}_1^{alg} - \mathbb{C}_M^{alg}) : \Delta\bar{\boldsymbol{a}} \tag{5g}$$

$$\bar{\mathbb{C}}^{alg} = \left[v_1\mathbb{C}_1^{alg} : \mathbb{B} + (1 - v_1)\mathbb{C}_M^{alg}\right] : [(1 - v_1)\mathbb{I} + v_1\mathbb{B}]^{-1} \tag{5h}$$

The Equation 5 summarizes the sequence of operations needed to calculate the homogenized algorithmic tensor $\bar{\mathbb{C}}^{alg}$, responsible for assigning at the material macroscopic point a total stress increment $\Delta\bar{\boldsymbol{\sigma}}$ from the known strain increment $\Delta\bar{\boldsymbol{\epsilon}}$. This procedure depends on each phase unique consistent algorithmic operator $\mathbb{C}_i^{alg}$. The regularization proposed in Doghri et al. [9] aims for the uniqueness of this operator. In addition, it was mentioned that these tensors should be isotropic for application of the analytical tensor $\mathbb{B}(\nu_M, v_1, Z)$. Isotropy ensures that the 3D problem can be represented by matrix Poisson's ratio ν_M. Uniformity allows the substitution of inclusions domain by volumetric fraction v_1 and their same specific spheroidal geometry by the aspect ratio Z.

$$\tilde{\mathbb{C}}_{n+1}^{alg} = \tilde{\mathbb{C}}_{n+1}^{vep} + \left(\tilde{\mathbb{C}}_{n}^{alg} - \tilde{\mathbb{C}}_{n+1}^{vep}\right) e^{\left(-\frac{h_{vepd,n+1}}{h_{vevpd,n+1} - h_{vepd,n+1}}\right)} \tag{6a}$$

$$\tilde{\mathbb{C}}_{n+1}^{vep} = \hat{\mathbb{C}}_{n+1}^{ve} - \frac{(2\hat{\mathcal{G}})^2}{h_{vepd,n+1}}\boldsymbol{N}_{n+1} \otimes \boldsymbol{N}_{n+1} \tag{6b}$$

$$\dot{p} = g = \frac{\omega(f_{n+1})}{(1 - D_{n+1})\eta_{vp}} \tag{6c}$$

$$h_{vepd,n+1} = -\frac{\partial_p g}{\partial_{\sigma_{eq}} g} \tag{6d}$$

$$h_{vevpd,n+1} = \frac{1}{\Delta t \partial_{\sigma_{eq}} g} - \frac{\partial_p g}{\partial_{\sigma_{eq}} g} \tag{6e}$$

A linear axial vicoplasticity model with isotropic hardening was explored by Doghri to develop a regularization method and by analogy extended it to a similar non-linear three-dimensional one. The Equation 6 already contains Miled et al. [7] contributions to include the linear viscoelastic model $\hat{\mathbb{C}}_{n+1}^{ve}$ and Krairi et al. [8] for damage. Therefore, it shows that the regularized tensor $\tilde{\mathbb{C}}_{n+1}^{alg}$ tends to a analytical viscoelastic-plastic operator $\tilde{\mathbb{C}}_{n+1}^{vep}$ if the time step Δt is small enough. As the authors themselves define, it is an interplay between analytical and numerical equations, so they also admits only the isotropic part of stiffness $\hat{\mathcal{G}}^{iso}$ and $\hat{\mathcal{K}}^{iso}$.

$$\mathbb{C}_{n+1}^{alg} = (1 - D_{n+1})\left(2\hat{\mathcal{G}}^{iso}\mathbb{I}^d + 3\hat{\mathcal{K}}^{iso}\mathbb{I}^v\right) \tag{7a}$$

$$\hat{\mathcal{G}}^{iso} = \frac{1}{10}\left(\mathbb{I}^d :: \tilde{\mathbb{C}}_{n+1}^{alg}\right) \tag{7b}$$

$$\hat{\mathcal{K}}^{iso} = \frac{1}{3}\left(\mathbb{I}^v :: \tilde{\mathbb{C}}_{n+1}^{alg}\right) \tag{7c}$$

2.3 Fatigue results

This section explore a very specific HDPE fatigue behavior case, limited to the mechanically dominated domain, as Janssen et al. [12] defined. Thus results are relevant only in the transition and high cycle fatigue regions of Wöhler curves. That limitation was a consequence of Krairi et al. [8] method for material parameters characterization and they are reproduced in Table 1 and Table 2. Macroscopic behavior is purely viscoelastic like the matrix phase, while inclusions have viscoplasticity and damage. If there is no other indication, the results are obtained with inclusions volume fraction $v_1 = 2\,\%$, spherical aspect ratio $Z = 1$, triangular shape fatigue loading, load frequency $f_s = 2\,Hz$, load ratio $R_s = 0$, hardening disabled and 50 time steps.

Table 1. Viscoelastic Parameters ([8])

$E_0 = 3000\,[MPa]$	$\nu_0 = 0.30$
$E_j\,[MPa]$	$\tau_j\,[s]$
981.5	0.01
500	80
611	0.036

In Figure 1 simulations results and reference Krairi et al. [8] curves were compared for maximum macro stress and damage evolution versus fatigue life N, as well the final average strain per cycle at $25MPa$ tensile maximum macro stress. Tensile and torsion predictive curves (a) show proximity with reference simulations and Zhang and Moore [13] experimental data, although we have less durability. Lower maximum stress damage evolution (b) and reference curve for $21\,MPa$ present same tendency to inflection and progressive distinction when that load decreases. Due to the regularization procedure, it is noted (c) a low dependence on the time step choice for the simulations. As expected, this approach converges according step decreases. Constitutive behavior (d) reaches to close reference final strain with a similar *ratchetting* effect.

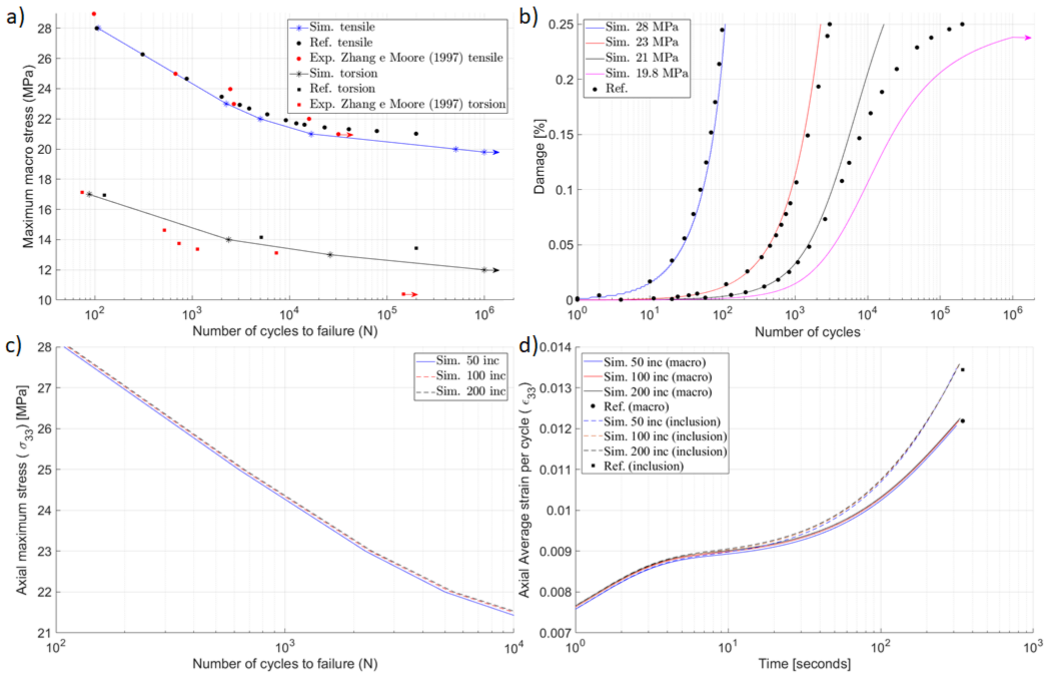

Figure 1. a) Wöhler curves under tensile and torsion fatigue load; b) Damage evolution in the weak spots under different maximum macro-stress tensile load; c) Time step sensibility study for a fixed tensile load; d) Average axial strain per cycle for three increment sizes under cyclic tensile $25\,MPa$ maximum stress; Reference Krairi et al. [8].

The dependence of fatigue response to the characteristics of the cyclic signal was studied with the present model and the results are displayed in Figure 2. The obtained results are in consonance to those described experimentally in Mortazavian et al. [14], an increase in frequency load results a longer fatigue life (b). Although the model is isotropic, also with $R_s = -1$ we expected the fatigue regimes transition but it was not observed. Simulation's case with frequency $f_s = 2\,Hz$ and load ratio $R_s = -1$ has twice strain rate of same frequency case and $R_s = 0$. As the frequency effect can be expected that change to $R_s = -1$ was increases the durability. On the other hand revers loading increase alternating stress compared to same maximum stress and $R_s = 0$. The sinusoidal shape has a lower average deformation rate per cycle, resulting in shorter fatigue life.

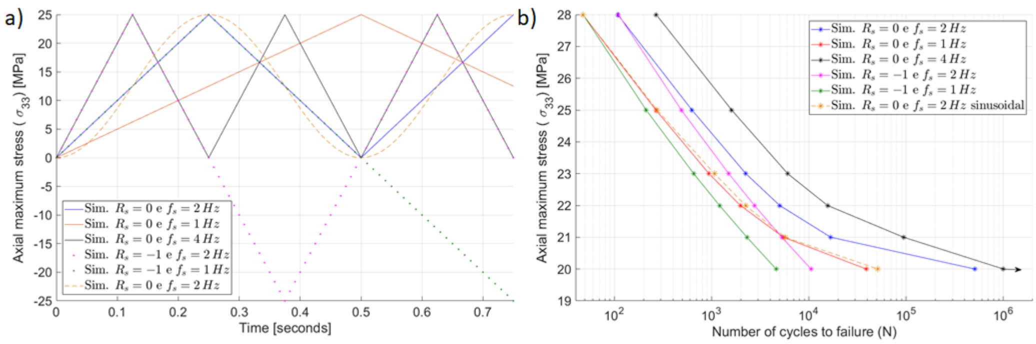

Figure 2. a) Tensile load with different frequency f_s and ratio R_s; b) Wöhler curves under (a) tensile fatigue load.

Table 2. Viscoplastic and damage Parameters ([8])

Initial yield stress	Isotropic hardening		Norton's Law	
$\sigma_{y0} = 7\,[MPa]$	$\kappa = 0\,[MPa]$	$n = 0\,[-]$	$\eta = 29x10^6\,[MPa \cdot s]$	$m = 6.2\,[-]$
		Damage		
$S = 0.02\,[MPA \cdot s^{-1}]$	$s = 2.3\,[-]$		$p_D = 0.0\,[-]$	$D_c = 25\%\,[-]$

The Figure 3 shows how the model response to variations on the material parameters σ_{y0} and damage module S. Three tests were run for each case considering increments of 10% on the parameter value. Initial yield stress σ_{y0} present directly relation with fatigue's life (a), more evident under higher maximum stress values. Considering this variation, the parameter σ_{y0} has significant influence on the low cycle regime and less for high cycles. The opposite is observed when the damage module S is evaluated. Large variations are observed in the number of cycles until failure, as long as the maximum stress decreases. It implies that the damage parameter S has capacity to adjust regime transition easier than viscoplatic parameter σ_{y0}.

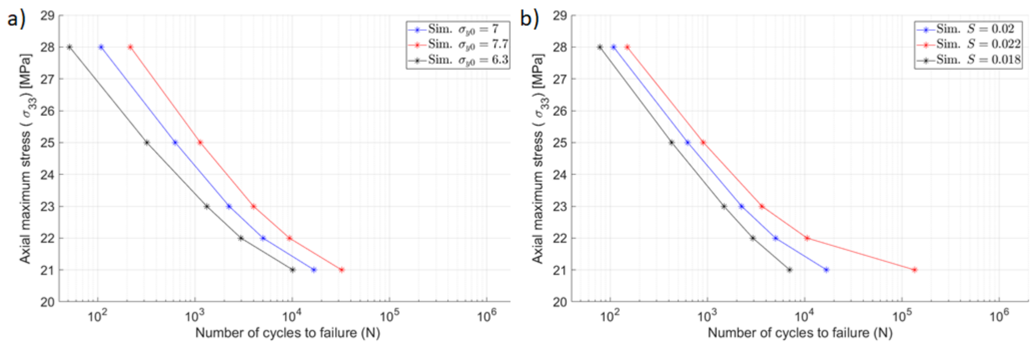

Figure 3. a) Initial yield stress σ_{y0} sensibility under tensile loading; b) Damage module S sensibility under tensile loading;.

3 Conclusions

This paper shows the implementation of a numerical model for fatigue estimation based on mean field homogenization procedures over a RVE composed of a viscoelastic phase and viscoelastic-viscoplastic dammaging inclusions. The obtained results were compared to those reported by Krairi et al. [8]. We found that our Wöhler curves and average final strain value are close to those reported results. The model seems to have great predictive capabilities for frequency changes and alternating stress effect. Preliminary results show the regime change inflection absence in $R_s = -1$ case. Some anisotropy can be add to improve this effect prediction. Sensitivity analysis studies show that the model presents capabilities for material parameters identification based on experimental data obtained at macroscopic level. Thus is convenient adjust the damage parameter S to extend the applicability for high cycle regime.

Acknowledgements. We want to thank all the GRANTE laboratory partners, especially the resources guaranteed by CAPES and the Federal University of Santa Catarina.

Authorship statement. The authors hereby confirm that they are the sole liable persons responsible for the authorship of this work, and that all material that has been herein included as part of the present paper is either the property (and authorship) of the authors, or has the permission of the owners to be included here.

References

[1] Teoh, S., 2000. Fatigue of biomaterials: a review. *International journal of fatigue*, vol. 22, n. 10, pp. 825–837.

[2] Mulla, Y., Oliveri, G., Overvelde, J. T., & Koenderink, G. H., 2018. Crack initiation in viscoelastic materials. *Physical review letters*, vol. 120, n. 26, pp. 268002.

[3] Bessell, T., Hull, D., & Shortall, J., 1975. The effect of polymerization conditions and crystallinity on the mechanical properties and fracture of spherulitic nylon 6. *Journal of Materials Science*, vol. 10, n. 7, pp. 1127–1136.

[4] Bretz, P. E., Hertzberg, R. W., & Manson, J., 1981. Mechanisms of fatigue damage and fracture in semi-crystalline polymers. *Polymer*, vol. 22, n. 9, pp. 1272–1278.

[5] Mura, T., 2013. *Micromechanics of defects in solids*. Springer Science & Business Media.

[6] Masson, R., Bornert, M., Suquet, P., & Zaoui, A., 2000. An affine formulation for the prediction of the effective properties of nonlinear composites and polycrystals. *Journal of the Mechanics and Physics of Solids*, vol. 48, n. 6-7, pp. 1203–1227.

[7] Miled, B., Doghri, I., Brassart, L., & Delannay, L., 2013. Micromechanical modeling of coupled viscoelastic–viscoplastic composites based on an incrementally affine formulation. *International Journal of solids and structures*, vol. 50, n. 10, pp. 1755–1769.

[8] Krairi, A., Doghri, I., & Robert, G., 2016. Multiscale high cycle fatigue models for neat and short fiber reinforced thermoplastic polymers. *International Journal of Fatigue*, vol. 92, pp. 179–192.

[9] Doghri, I., Adam, L., & Bilger, N., 2010. Mean-field homogenization of elasto-viscoplastic composites based on a general incrementally affine linearization method. *International Journal of Plasticity*, vol. 26, n. 2, pp. 219–238.

[10] Krairi, A. & Doghri, I., 2014. A thermodynamically-based constitutive model for thermoplastic polymers coupling viscoelasticity, viscoplasticity and ductile damage. *International Journal of Plasticity*, vol. 60, pp. 163–181.

[11] Pierard, O., Friebel, C., & Doghri, I., 2004. Mean-field homogenization of multi-phase thermo-elastic composites: a general framework and its validation. *Composites Science and Technology*, vol. 64, n. 10-11, pp. 1587–1603.

[12] Janssen, R. P., de Kanter, D., Govaert, L. E., & Meijer, H. E., 2008. Fatigue life predictions for glassy polymers: a constitutive approach. *Macromolecules*, vol. 41, n. 7, pp. 2520–2530.

[13] Zhang, C. & Moore, I. D., 1997. Nonlinear mechanical response of high density polyethylene. part i: Experimental investigation and model evaluation. *Polymer Engineering & Science*, vol. 37, n. 2, pp. 404–413.

[14] Mortazavian, S., Fatemi, A., Mellott, S. R., & Khosrovaneh, A., 2015. Effect of cycling frequency and self-heating on fatigue behavior of reinforced and unreinforced thermoplastic polymers. *Polymer Engineering & Science*, vol. 55, n. 10, pp. 2355–2367.